# ON MULTI-OBJECTIVE OPTIMIZATION OF PLANETARY EXPLORATION ROVERS APPLIED TO EXOMARS-TYPE ROVERS

ESA/ESTEC, NOORDWIJK, THE NETHERLANDS / 12 – 14 APRIL 2011

Alexandre Carvalho Leite [(1)], Bernd Schäfer [(2)]

[(1)] Currently at DLR – Germany as Guest Scientist from Instituto Nacional de Pequisas Espaciais (INPE) – Brazil, Münchner Straße 20, 82234 Weßling, Germany, alexandre.carvalholeite@dlr.de.
[(2)] German Aerospace Center (DLR), Münchner Straße 20, 82234 Weßling, Germany, bernd.schaefer@dlr.de.

ABSTRACT

ExoMars is the first robotic mission of the Aurora program of the European Space Agency (ESA). Surface mobility (as provided by ExoMars rover) is one of the enabling technologies necessary for future exploration missions. This work uses previously developed mathematical models to represent an ExoMars rover operating in soft/rocky terrain. The models are used in an optimization loop to evaluate multiple objective functions affected by the change in geometrical design parameters. Several objective functions can be used in our optimization environment powered by MOPS (Multi-Objective Parameter Synthesis). Two environments are used to simulate the rover in stability sensitive conditions and power and sinkage sensitive conditions. Finally, an ExoMars-like configuration is proposed and consistent improvement directions are pointed out.

## 1. INTRODUCTION

In 2001 the ESA set up the Aurora programme as part of the Europe's strategy for space [5]. The step-by-step approach of the Aurora programme includes robotic exploration, and ExoMars is the first robotic mission of the Aurora program. Fig. 1 illustrates the two missions foreseen within the ExoMars programme. In 2016 a mission with an Orbiter plus an Entry, Descent and Landing demonstrator and 2018 with two rovers, [10].

Surface mobility is one of the enabling technologies necessary for future exploration missions. A powerful planetary six-wheeled rover (ExoMars rover) is being developed for this purpose. It is called an all-terrain rover and has a simple kinematic structure composed of three independent bogies (each with two wheels attached). The six-wheeled kinematic structure should provide safe and efficient mobility to a heavier payload.

The vehicle will face complex shaped obstacles (rocks), rough terrain with pebbles and sand making the locomotion task even more challenging. Slippery behavior of the driving wheels, excessive sinkage and steep traversing are real driving conditions of the vehicle.


Figure 1. ExoMars missions (2016 and 2018).

This work uses previously developed mathematical models to represent an ExoMars rover operating in soft/rocky terrain, [8] and [7]. These models are used to synthesize a high performance lightweight configuration of the ExoMars rover. The models can be essentially classified as: environment, vehicle and their interaction. Environment models are the relief pattern of an undulating terrain, deformation of the terrain (in case of sand) and complex shaped stones. The vehicle is modeled as a Multi-Body System (MBS) with standard rigid connections and rotational joints. They interact with each other through contact models based on Bekker's equations for sand and coulomb friction for stones and bedrocks.

The models are used in an optimization loop to evaluate multiple objective functions affected by the change in geometrical design parameters. This approach is presented in the sequence as an attempt to improve even more the performance of ExoMars-type rovers in all-terrain navigation.

## 2. MODELING AND SIMULATION

We developed an optimization environment relying on Multi-Body System simulation models and contact

dynamics. The MBS models can be changed according to the suspension to be optimized, and the contact models are parameterized for each specific terrain characteristic. Our modelling/simulation environment is Dymola, where the MBS diagrams and force elements of the contact models are implemented in Modelica and external libraries respectively, see Fig. 2. For details on the implemented contact dynamics, we refer the interested reader to [8].

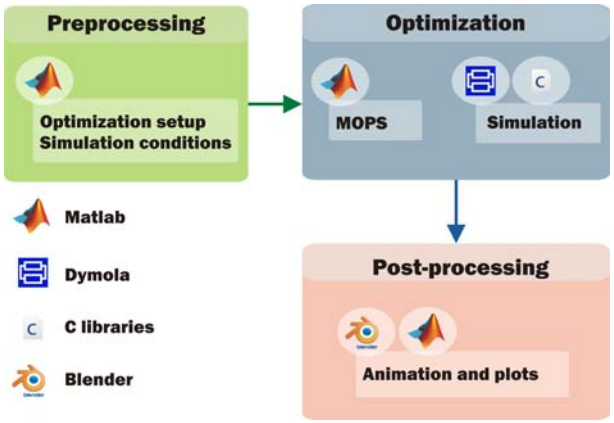


Figure 2. Overview of the rover optimization tool, [11]

Once a rover's suspension is modelled, terrain characteristics like stones and sand can be added to the simulation model and properly configured to represent a certain driving scenario. Friction coefficient of the stones, distribution and quantity of stones at the planetary surface terrain, Bekker parameters [1] of the soft soil, and relief pattern of the landsite are examples of characteristics which can be changed to fit a representative driving scenario.

Figure 3. Animation comparing two configurations of ExoMars rover on a rocky rigid terrain

Pre-processing is employed in order to speed up the generation of new terrain characteristics. New scenarios and simulation models can be generated with the help of the pre-processing, where a smooth relief pattern can be assigned to the landsite and complex-shaped stones can be generated and stochastically placed on that terrain. The simulation model generated is quite complex, some tuning parameters are required to assure the stability of the simulations [9]. Note that parameters of the suspension (modelled as a MBS model) are intended to be changed by an optimizer; the parameters set regarding the terrain, characterize different optimization scenarios; and the tuning parameters are changed only in case of numerical instability of the simulation.

Optimization runs inside Matlab were standalone compiled Dymola models are executed. The results of each optimization step (equivalent to a simulation run) can be viewed in post-processing phase. The simulations can be rendered and visualized in animation movies (see Fig. 3), bar plots and parallel coordinates are also available to show the improvements.

## 3. MULTIPLE OBJECTIVE OPTIMIZATION

Several objective functions can be used in our optimization environment powered by MOPS (Multi-Objective Parameter Synthesis). MOPS is an in-house software optimization tool developed at DLR, it implements various optimization methods in order to achieve a satisfactory solutions' set in the multi-objective space, see Fig. 4. It is used in Matlab environment.

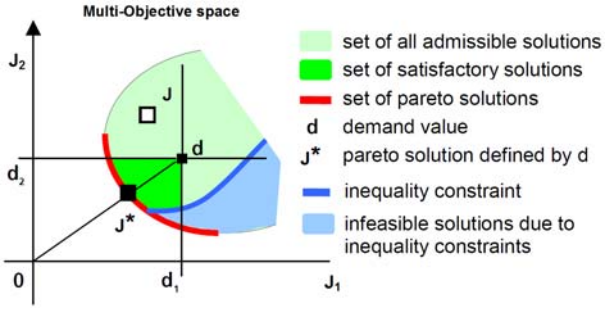


Figure 4. Min-max multi-objective optimization, [6].

In the following subsection we describe some relevant objective functions used in the optimization of all-terrain wheeled rovers. They are: overall mass, average consumed power, accumulated sinkage and dynamic stability. Subsequently, the scaling and aggregation of objective functions is briefly commented.

### 3.1. Description of objective functions

Overall mass $(J_M)$

The overall mass of the rover is the simplest objective function; it is simply defined as the sum of the mass of each rigid body $m_k$ in the rover, including payload.

$$J_M = \sum_{k=1}^{num\,of\,bodies} m_k \quad (1)$$

This objective function is static and does not need a dynamic simulation to be evaluated. But it constrains the solution to a lightweight design, or at least lighter than the current design. It is to be used in combination with other objective functions and limitations in the design parameters variation, otherwise it goes to zero.

Average consumed power $(J_P)$

One of the purposes of our work is to achieve efficient designs, they should be able to travel mission planned distances with low battery consumption. The average consumed power is computed for each wheel regarding the simulation time ($t_{sim}$). Finally, the individually computed powers of each wheel are summed up

$$J_P = \sum_{i=1}^{number\,of\,wheels} \frac{1}{t_{sim}} \int_0^{t_{sim}} \tau_i \cdot \omega_i dt \quad (2)$$

where $\tau_i$ and $\omega_i$ are torque and angular velocity of the $i^{th}$ wheel.

Accumulated sinkage $(J_S)$

Sinkage is a very important measure of the dynamic behaviour of a vehicle in soft soil. It is a measure of a mission critical situation, where the rover digs excessively the soil and becomes motionless or with high slippage. But it is also a measure of driving efficiency in soft soil, because the unprepared soil must be compacted so that the wheel achieves sufficient thrust. Compaction is equivalent to the vertical work per unit length in pressing a wheel into the ground to a depth of its maximum sinkage [5]. Thus, we use sinkage volume per travelled distance to measure driving efficiency in soft unprepared terrain:

$$J_S = \frac{V_S}{\sum_{i=1}^{number\,of\,wheels} d_i^{trav}} \quad (3)$$

where $V_S$ is the sinkage volume, calculated at the end of a simulation. The volume integral is computed over the tangential coordinates of the inertial frame as illustrated in the elevation model of a wheel footprint in soft terrain in Fig. 5.

The travelled distance $d^{trav}$ is computed as the integral of the forward velocity of each wheel only when it is in contact with soft ground.

$$d^{trav} = \int_0^{\Delta t} \left( v_{fwd} \cdot c_g \right) dt \quad (4)$$

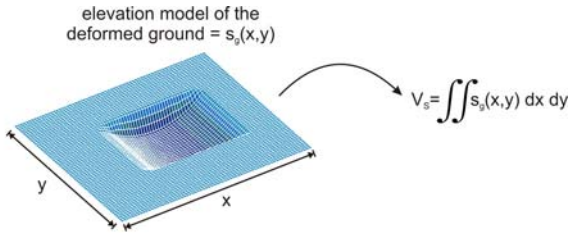


Figure 5. Computation of $V_S$ in deformed terrain.

Forward velocity $v_{fwd}$ and ground contact flag $c_g$ are defined as follows

$$v_{fwd} = -\boldsymbol{v}_0 \cdot \boldsymbol{e}_{long} \quad (5)$$

$$c_g = \begin{cases} 0, & \textit{if no contact with the ground} \\ 1, & \textit{otherwise} \end{cases} \quad (6)$$

where $\boldsymbol{v}_0$ is the translational velocity vector of the wheel in the inertial frame, and $\boldsymbol{e}_{long}$ is the longitudinal unity vector of the wheels' reference contact point also in the inertial frame.

Sinkage is highly sensitive to geometric characteristics of the wheel and to interaction dynamics between a specific soil and the rover. Note that the slip behaviour is partially captured in this measure by $d^{trav}$.

Dynamic stability $(J_D)$

Static stability is an important issue taken into account in a rover's design phase. But static indeterminacy problems and the large configurations which can be assumed by a complex suspension of the vehicle restricts the analysis. On the other hand, through dynamic simulation it is possible to compute the normal forces on each contact point of the wheels and evaluate several configurations of the suspension when the rover drives over rocks with different shapes and sizes. The position of the wheels and the normal forces in its contact points can be used to compute the "Force-Angle Stability Measure" $\alpha$ presented in [4]. We used this measure to compute the worst situation after a dynamic simulation of a rover driving on a rough terrain,

$$J_D = \min(\pi - \alpha) \quad (7)$$

The overall Force-Angle Stability measure is given by

$$\alpha = \min\left(\theta_j\right)\frac{\|\boldsymbol{f}_r\|}{\|\boldsymbol{f}_n\|}, \quad j = \{1,\ldots,n_{cp}\} \tag{8}$$

where $-\pi \le \theta_i \le \pi$ is the angle measure associated with the $j^{th}$ tipover axis, $\boldsymbol{f}_r$ is the net force acting on the center of mass of the vehicle, $\boldsymbol{f}_n$ the normal force used for normalization of the measure and $n_{cp}$ is the number of contact points with the ground or stones. The outermost wheel contact points $\boldsymbol{p}_j$ which form a convex polygon on the horizontal plane are connected through lines referred as tipover axes $\boldsymbol{a}_j$. The normal vector $\boldsymbol{l}_j$ of a tipover axis is used to compute the angle measure as

$$\theta_j = \sigma_j \cos^{-1}\left(\hat{\boldsymbol{f}}_r \cdot \hat{\boldsymbol{l}}_i\right) \tag{9}$$

with

$$\sigma_j = \begin{cases} +1, & \text{if } \left(\hat{\boldsymbol{l}}_j \times \hat{\boldsymbol{f}}_r\right)\cdot\hat{\boldsymbol{a}}_j < 0 \\ -1, & \text{otherwise} \end{cases} \tag{10}$$

Fig. 6 shows the contact points of the wheels of a rover and its support polygon in the geometry of the Force-Angle Stability Measure.

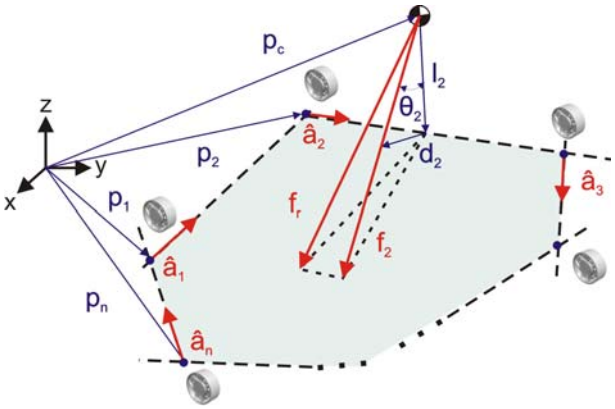


Figure 6. Geometry of the Dynamic Stability Measure

### 3.2. Scaling and Aggregation Functions

Since objectives functions must be compared during the optimization process, they are scaled over a range of meaningful values similar to fuzzy membership functions, where numeric values of the feasible range of objective functions are assigned to linguistic values like *bad* and *good*. These scaled objective functions must lie in the acceptable range, i.e. between the demand value and the optimal value. Fig. 7 illustrates the idea.

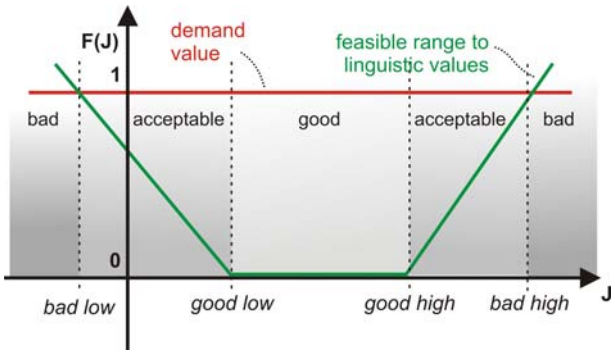


Figure 7. Scaling of the objective functions

Hence the multiple objective functions can be assembled into a unique expression. This expression is called aggregation function and is evaluated at each step of the optimization method. The aggregation function $\Gamma$ strongly influences the convergence of the solution and can be viewed as an additional tuner of the design optimization process. We used the following aggregation functions in this work

$$\Gamma_1 = \min \max_{g\in\{M,P,S,D\}} \left\{F_g\left(J_g\right)/w_g\right\} \tag{11}$$

$$\Gamma_2 = 1/2 \sum_{g\in\{M,P,S,D\}} \left[F_g\left(J_g\right)/w_g\right]^2 \tag{12}$$

where $w_g$ is the demand value used to weight the corresponding scaled objective function.

## 4. OPTIMIZATION SCENARIOS

There are several interesting situations (driving conditions and landing sites) to simulate and optimize a rover's design. Although, this task can be time consuming; because a single highly representative terrain (with several complex shaped rocks and uneven soft terrain) needs few minutes to be simulated. Another drawback is that there is no guarantee that the vehicle will explore all characteristics of the terrain. Slight modifications in the initial conditions of the simulation can give completely different results, like divergent driving paths.

We noted that highly representative terrains are useful to evaluate the synthesized solution(s) and perform trade-off between two or more satisfactory designs. We also noted that simple optimization scenarios can be used in the optimization process. These simple optimization scenarios are capable of enforce the vehicle to face exactly that critical situation to which it must be optimized. Nevertheless, short simulation times are sufficient to perform the intended performance evaluation.

In this work we used two simple optimization scenarios: 1) sandy plane with one stone; 2) irregular downhill

(rigid terrain).

**4.1.** Sandy plane with one stone

In this scenario, the same complex shaped stone is always placed in the same relative position to the front right wheel of the rover. The plane is deformable according to our contact models and allows multipass effects to the following wheels, see Fig. 8.

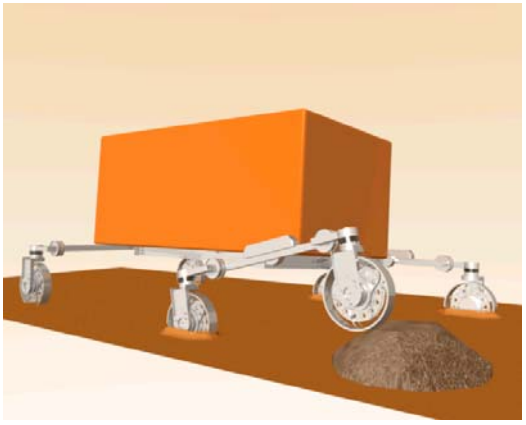

Figure 8. Scenario 1: sandy terrain with stone

The vehicle will hardly face a *bad* value of dynamic stability measure, but average consumed power and accumulated sinkage can be suitably evaluated.

**4.2.** Irregular downhill (rigid terrain)

This scenario was conceived to compensate the weakness of the previous scenario. The rover starts with the front right wheel on the complex shaped stone, but on a plane. When it drives straight ahead the front wheels step down onto a -20º ramp, see Fig. 9.

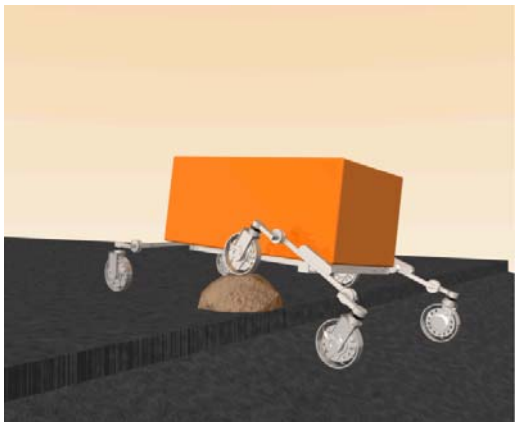

Figure 9. Scenario 2: bedrock with stone, step down and downhill

Note that this scenario will always demand resilience of the suspension system and therefore substantial changes in the dynamic stability measure. Average consumed power is not of concern in this scenario and accumulated sinkage is not applicable in rigid terrain.

## 5. EXOMARS-TYPE ROVER OPTIMIZATION

Some geometric properties of the rover's suspension (locomotion subsystem) are assumed as design parameters (Fig. 10), i.e. they can be changed during the optimization process to achieve desirable values of the objective functions.

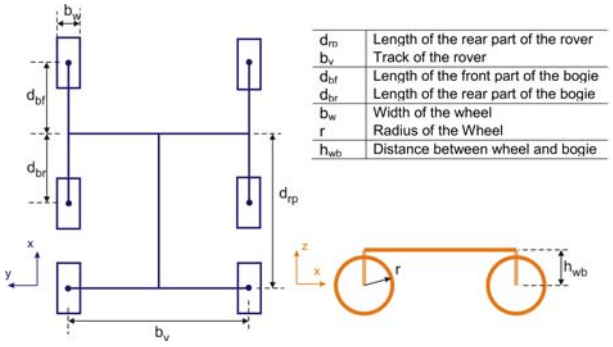


Figure 10. Geometric design parameters in ExoMars suspension

The objective functions are scaled according with *bad-good* scaling shown in Fig. 7, the configuration of each scaling profile is given in Tab. 1.

Table 1. *Bad-good* scaling parameters

| **Obj. Fcn** | ***Bl*** | ***Gl*** | ***Gh*** | ***Bh*** |
|---|---|---|---|---|
| $J_M$ | - | - | 75kg | 85kg |
| $J_P$ | - | - | 5.0W | 6.4W |
| $J_S$ | - | - | 0.5l/m | 0.65l/m |
| $J_D$ | - | - | 3rad | 5.5rad |

Bl – Bad low, Gl – Good low. Gh – Good high, Bh – Bad high.

Arbitrary high values are assigned to the objective functions when a simulation failure occurs. It causes discontinuities in those exceptional cases and disturbs optimization. MOPS provides a mechanism to handle criteria with exceptional cases so that it guaranties that the discontinuities remain small in those cases.

There are several optimization methods available in MOPS, in this work we used the genetic algorithm based on the evolution strategies of [2].

**5.1.** First example: stability/mass optimization

This example shows how a stable rover with reduced mass is synthesized. Note that these two needs will precisely require two objective functions: $J_M$ (static) and $J_D$ (dynamic). Only one scenario (irregular downhill) is sufficient to evaluate the single dynamic objective function. The aggregation function used was $\Gamma_1$ with demand values $d_M = 0.8$ and $d_D = 1$, i.e. mass reduction is the most important objective function.

Table 2. Nominal and optimal configuration

| | | |
|---|---|---|
| **Nominal** | 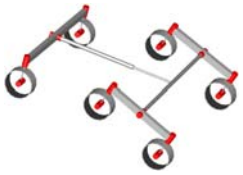 | $r$ = 0.125m<br>$b_w$ = 0.1m<br>$d_{bf}$ = 0.32m<br>$d_{br}$ = 0.32m<br>$d_{pr}$ = 1.08m<br>$b_v$ = 1.27m<br>$h_{wb}$ = 0.205m |
| **Optimized** | 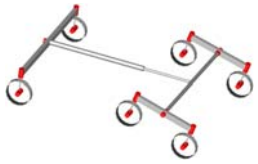 | $r$ = 0.133m<br>$b_w$ = 0.053m<br>$d_{bf}$ = 0.32m<br>$d_{br}$ = 0.32m<br>$d_{pr}$ = 1.52m<br>$b_v$ = 1.45m<br>$h_{wb}$ = 0.21m |

The improvement in stability was significant, one can see in Tab. 2 that the convex support polygon is increased by the outermost contact points of the optimal configuration. Although the mass reduction was not significant, because increasing the track or bogie length will achieve better values of $J_D$ but consequently increase the overall mass of the vehicle. The achieved improvements are those on Fig. 11.

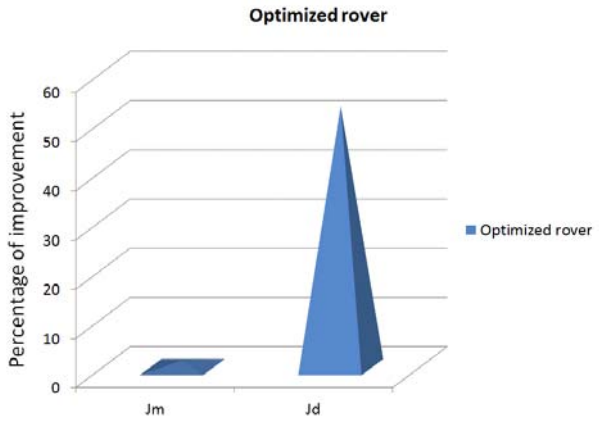


Figure 11. Percentage of improvement upon the nominal

It is possible to increase the weight of $J_M$ inside the aggregation function but this strategy deteriorates the dynamic stability and also static stability by reducing the track of the vehicle. This example gives us a reasonable insight of the problem, which constrains the desirable solution space around the nominal configuration.

**5.2.** Second example: stability, mass, average power and accumulated sinkage optimization

This example needs two scenarios to evaluate the four objective functions. As noted before, we are not expecting solutions which deviate so much from the nominal configuration. Additionally a two-step procedure was employed as an optimization strategy:

1 The entire structure was optimized constraining $d_{bf} = d_{br}$.
2 A new optimization was carried out allowing only those two parameters to be changed, but constraining the front bogies' length as having always the same value as given by the previous step.

The results of each step are listed in Tab. 3.

Table 3. Results of two-step optimization

| | | |
|---|---|---|
| **Optimal: Step 1** | 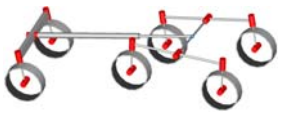 | $r$ = 0.163m<br>$b_w$ = 0.09m<br>$d_{bf}$ = 0.395m<br>$d_{br}$ = 0.395m<br>$d_{pr}$ = 1.42m<br>$b_v$ = 0.65m<br>$h_{wb}$ = 0.242m |
| **Optimal: Step 2** |  | $r$ = 0.163m<br>$b_w$ = 0.09m<br>$d_{bf}$ = 0.28m<br>$d_{br}$ = 0.51m<br>$d_{pr}$ = 1.42m<br>$b_v$ = 0.65m<br>$h_{wb}$ = 0.242m |

Note in Fig. 12 that the achieved improvements are not easy to compare with each other. The dynamic stability of the solution of step one is worse than that of the nominal rover, but with improvements in accumulated sinkage and power saving. The consumed average power of the solution of the step two is worse than that of the nominal rover, but with a much better dynamic stability. In both solutions the mass is the same with a slighter improvement, because the only difference is the location of the pivot of the front bogies. Two objective functions ($J_P$ and $J_D$) are very sensitive to this parameter. In the next section, the variation of this parameter is performed to investigate its optimization potential.

**5.3.** Lateral pivots location and bending constraint

We adopted the pivot location parameter as being $\left[d_{bf} \middle/ \left(d_{bf} + d_{br}\right)\right] \times 100\%$. The reference configuration is the nominal rover (first row in Tab. 2). Two extreme values were chosen as test values for the length of the bogie $d_{bf} + d_{br} = 0.4\text{m}$ and $d_{bf} + d_{br} = 0.8\text{m}$. Fig. 13

shows the dynamic stability values for each configuration of the nominal rover with different pivot locations in two bogie lengths. A plane with the nominal value of the dynamic stability measure is used as reference.

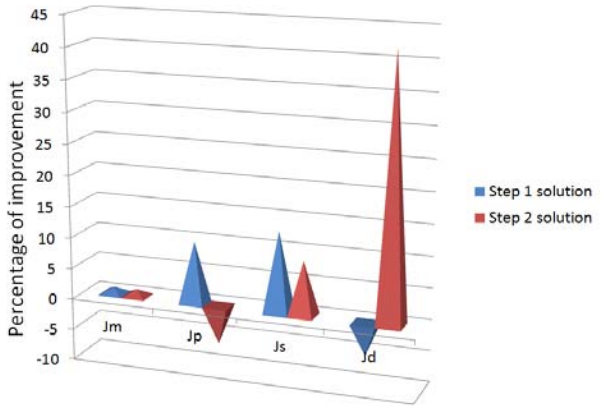


Figure 12. Percentage of improvement upon the nominal

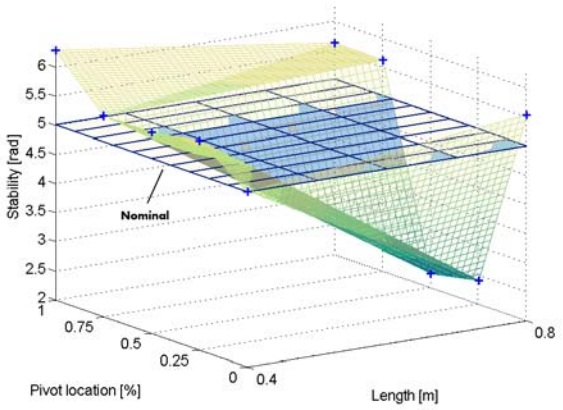


Figure 13. Dynamic stability measure as a function of bogie length and pivot location in scenario 2

When the pivot is located exactly at one of the wheels' steering axis, dynamic stability is prejudiced. The reason is that the normal force distribution becomes excessively imbalanced. Reasonable values are found about the geometrical centre of the bogie. Stability improvement is not the only advantage in changing the pivot location; thinner bogies can be used in this case because the maximal deflection of the beam is decreased for the same load.

The maximal bending moment is smaller for other locations around the geometric centre of the bogie, this allows the choice of thinner bogies and consequently lighter. This additional parameter (cross sectional area constrained by the maximal bending moment) is strongly coupled with $J_M$ and weakly coupled with $J_D$. A simple analysis based on Euler-Bernoulli beam theory can be applied to get better results from the automatic synthesis given in Tab. 3. The relationship between width and height of the rectangular cross section of the beam remains $height = 1.5 \times width$ like in the nominal configuration. Equation 13 computes width of the beam for $pivot\,location = 0\%$ and equation 14 for $pivot\,location \neq 0\%$.

$$b_c^4 = \frac{P\left(d_{bf} + d_{br}\right)^3}{w_{\max} E \times 13.5} \tag{13}$$

$$b_c^4 = \frac{\sqrt{3} P d_{bf} \left(\left(d_{bf} + d_{br}\right)^2 - d_{bf}^2\right)^{3/2}}{w_{\max} E \left(d_{bf} + d_{br}\right) \times 7.59} \tag{14}$$

$E$ is the elastic modulus, $w_{\max}$ is the maximum allowed deflection computed with the reference values of the nominal configuration, $P$ is the vertical load applied by the payload on its connection with the bogie and $b_c$ is the width of the rectangular cross section of the beam.

Fig. 14 shows the mass reduction acquired by this approach.

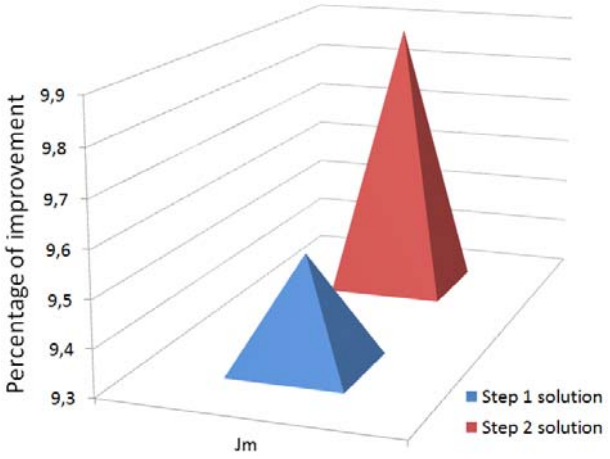


Figure 14. Mass reduction improvement

${}^{Step1}J_M = 84.85\text{kg}$ and ${}^{Step2}J_M = 84.51\text{kg}$ compared with ${}^{Nominal}J_M = 93.8\text{kg}$

Reasonable constraining specifications are currently in research to specify bending constraints for a rover driving on a rough terrain, instead of a simple three-point bending model based on shock loads applied on a single point. This is the reason because this approach is not yet implemented in the automatic optimization loop.

## 6. CONCLUSION AND COMMENTS

An optimization tool was presented in this work, including modelling and simulation environment, multi-objective optimization facility, specific objective functions for planetary rovers and visualisation. The

study case is the ExoMars-type suspension, where a nominal configuration was taken as reference to be optimized.

In the first example the rover was optimized for a specific terrain suitable for dynamic stability evaluation. Significant results were achieved for dynamic stability improvement, but mass reduction was insignificant. This example shows the difficulty to synthesize a lightweight rover with good dynamic stability characteristics. The main difficulties are: 1) the narrow range which the design parameters are allowed to vary to cope with other design specifications (e.g. ground clearance); 2) mass and stability are strongly coupled and conflicting.

In the second example, average consumed power and accumulated sinkage are also inserted as objective functions in the optimization process. A two-step procedure was adopted as a strategy to synthesize an all-terrain optimal rover. The output of the process was a rover with improvements in all objective functions except consumed power, which can be approached by optimal control. Mass reduction can also be significantly improved when bending moment constraints are taken into account to re-size the cross sectional area of the rear and front bogies.

We would like to summarize the following directive measures for further improvements in mass reduction and power saving:

1 Bending moment constraints for feasible mass reduction of the bogies.
2 Changes in the wheel design to get lighter wheels without deteriorating the performance in soft soil and surmounting rocks.
3 Optimal control to achieve efficient behavior.

From our experience, the first directive measure is sufficient to achieve power saving in geometric design parameters' level. The second can be implemented without changes in the contact models, allowing several shapes (not only toroid or cylinder wheels). Optimal control would only be applied as a last optimization step and not concurrently with the optimization of the mechanical structure.

## **7.** ACKNOWLEDGEMENT

Financial support from the German Academic Exchange Service (Deutscher Akademischer Austausch Dienst - DAAD) is gratefully acknowledged.

## **8.** REFERENCES

1. Bekker, M. G. (1956). Theory of Land Locomotion. The University of Michigan Press, USA.

2. Goldberg, D. E. (1989). Genetic Algorithms in Search, Optimization and Machine Learning. Addison-Wesley, Reading, Massachusetts, USA.

3. Papadopoulos, E. G. & Rey, D. A. (1996). A new measure of tipover stability margin for mobile manipulators. In IEEE International Conference on Robotics and Automation (ICRA'96). Minneapolis, USA.

4. Apostolopoulos, D. S. (2001). Analytical Configuration of wheeled robotic locomotion. PhD thesis, Carnegie Mellon University, Pittsburgh, Pennsylvania, USA.

5. ESA (2006). Aurora's origins. Online at http://www.esa.int/esaMI/Aurora/SEMZOS39ZAD_0.html (as of 4 April 2011).

6. Joos, H. H. (2008). Mops - multi-objective parameter synthesis user's guide v 5.3. Technical Report DLR IB 515-08-37.

7. Leite, A. C. & Schäfer, B. (2010). Multibody modeling and multi-objective optimization of a six-wheeled steerable vehicle and its motion controllers. In 1st ESA Workshop on Multibody Dynamics for Space Applications, Noordwijk, Netherland.

8. Leite, A. C. & Schäfer, B. (2010). A Comprehensive Wheel-Terrain Contact Model for Planetary Exploration Rover Design Optimization. The Joint 9th Asia-Pacific ISTVS Conference and Annual Meeting of Japanese Society for Terramechanics, Hokkaido, Sapporo, Japan.

9. Leite, A. C. & Schäfer, B. (2010). Mass, power and static stability optimization of a 4-wheeled planetary exploration rover. In 2nd International Conference on Engineering Optimization. Lisbon, Portugal.

10. ESA (2011). The ESA-NASA ExoMars programme 2016-2018 – an overview. Online at http://astronomy2009.esa.int/science-e/www/object/index.cfm?fobjectid=46048 (as of 4 April 2011).

11. Schäfer, B. & Leite, A. C. (2011). Development Environment for Optimized Locomotion System of Planetary Rovers. In 14th International Symposium on Dynamic Problems of Mechanics. São Sebastião, São Paulo, Brazil.